The operation of the LHCb RICH photon detection system in a charged particle test beam

Sean Brisbane
University of Oxford, Department of Physics, Oxford OX1 3RH, UK.
(on behalf of the LHCb RICH Collaboration)

Abstract

The LHCb experiment at CERN employs two Ring Imaging Cherenkov (RICH) detectors to provide particle identification over the range 1 to 100 GeV/c. The RICH detectors use custom-built Hybrid Photon Detectors (HPDs) to detect the Cherenkov photons over the wavelength range $200-600$ nm. Three columns of 16 HPDs with final readout electronics and data acquisition were installed in a prototype Cherenkov gas enclosure. Two gas radiators were studied, nitrogen and C_4F_{10}. Saturated Cherenkov rings ($\beta \approx 1$) were focused onto the plane of HPDs by exposing the radiators to a beam of 80 GeV/c charged pions from the CERN SPS, operated with a 25 ns bunch structure. The HPDs and the on- and off-detector electronics performed to specification, and the DAQ system was verified under the sustained 40 MHz readout mode required for LHC running. The analysis verified the local alignment across the HPDs and their relative timing. The photon yields from both radiators are in good agreement with expectations.

Key words: Ring Imaging Cherenkov detectors, Hybrid Photon Detectors, LHCb Experiment, RICH detector
PACS: 29.40.Ka

1. The LHCb RICH Detectors

The LHCb experiment at CERN will make precision measurements of CP violating phases in the quark sector and search for rare B decays [1][2]. In order to expand the range of hadronic modes available for detailed study, two Ring Imaging Cherenkov (RICH) detectors will be employed to provide $K-\pi$ separation over the momentum range $1-100$ GeV/c [3]. The upstream detector (RICH 1) will employ the Cherenkov radiators silica aerogel and gaseous C_4F_{10} and the downstream detector (RICH 2) will contain CF_4. Each respective radiator will provide discrimination between progressively higher momentum particles. In both RICHes, a combination of spherical and plane mirrors will focus the Cherenkov light-cones.

The Cherenkov radiation will be detected by arrays of Hybrid Photon Detectors (HPDs) [4], arranged into 14 columns each of 14 HPDs in RICH 1, and into 18 columns each of 16 HPDs in RICH 2. When combined with momentum information, the most likely particle hypotheses can be extracted.

2. Test Beam Setup

A set of three production columns of HPDs from RICH 2 were tested in a beam of 80 GeV/c negatively charged particles from the SPS accelerator at CERN. The columns were installed inside a light-tight aluminium gas vessel (see Fig. 1) containing a parabolic mirror with 1016 mm focal length and 200 mm diameter. The mirror could be adjusted to focus the photons emitted from a given track onto any of the central ten HPDs. The vessel presented a gas length of 1102 mm, and was filled first with ni-

trogen and then with C_4F_{10} through the course of the beam test. Nitrogen rings were contained within the acceptance of a single HPD whereas the C_4F_{10} rings could be chosen to spread over three or four HPDs, depending on the mirror alignment.

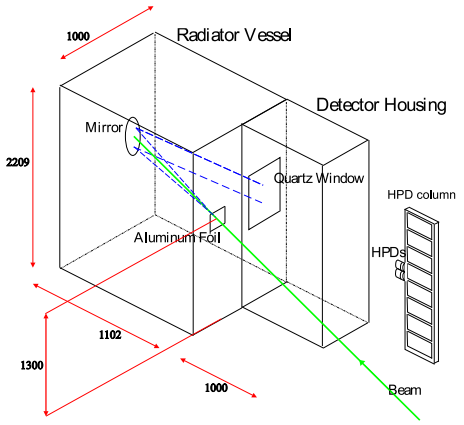

Fig. 1. A schematic overview of the RICH detector used in the beam test. The direction of the particle beam is indicated, the dashed lines represent the trajectories of the Cherenkov photons. All dimensions are in mm. To simplify the illustration, only one detector column with two HPDs is shown (three fully mounted columns were used during the beam test).

The HPD is described elsewhere [4], however the features relevant to the test beam data-taking are described below. Photo-electrons produced at the HPD photo-cathode are accelerated by a 20 kV cross-focusing electric field. The electrons are demagnified by a factor of five before striking a silicon-diode sensor subdivided into a 32×32 matrix of pixels each of area $500 \times 500\,\mu\text{m}^2$. The resulting granularity is 2.5×2.5 mm^2 at the HPD photo-cathode. A photo-electron incident on the sensor produces a signal of typically 5000 e^-/hole pairs, well above the mean noise level per pixel of around 150 electrons. Bump bonded onto the silicon sensor is an LHCBPIX1 CMOS binary readout chip [5] where the signal is digitised at 40 MHz and stored in one of 16 delay units for the duration of the 4 μs trigger latency.

A "Level-0" (L0) front-end board [6] controls the readout of the data from a pair of HPDs in 32×40 MHz streams per LHCBPIX1 chip, resulting in a maximum readout rate of 1 MHz. The data are serialised and sent via two Gigabit Optical Links to the "UKL1" [7] off-detector readout board, located outside the radiation area. The UKL1 formats and zero suppresses the data and passes the data to a readout network with identical architecture to be implemented in LHCb. Previous test-beam studies have been reported [8].

The SPS was configured to produce bunches of particles with 25 ns spacing, with identical bunch structure to be used in the LHC. The beam consisted of 90% π^- and e^-, for which the opening angle of the Cherenkov cone was saturated ($\beta \approx 1$) in the two radiators. The beam contained approximately a 10% contamination of K^- and $\bar{p}$. The intensity was tuned so that only 4% of non-empty bunches had more than one particle. Four coincident scintillators, two either side of the vessel, formed the synchronous trigger. The small size of the scintillators meant that the beam divergence for triggered events was limited to $\sim$1.5 mrad.

3. Time alignment

Bunches of particles arrived at the entrance window of the vessel at a well-defined phase with respect to the SPS machine clock. In order to demonstrate fully synchronised data taking at 40 MHz, the electronics components were configured to trigger on non-empty bunches. To ensure that there was no efficiency loss arising from the variation of pixel response times with signal pulse height, a fine time alignment was required. Fine-time adjustments on the L0 front-end boards were used to delay the clock signal to the LHCBPIX1 in 1 ns steps with respect to the SPS machine clock. The delay settings were incremented until the maximum detection efficiency for triggered events was reached across the HPD pixel array.

4. Photo-electron Yield Studies

The photo-electron yields were estimated with both nitrogen and C_4F_{10} radiators. Events with at least five hits recorded on the HPDs at the photon detector plane were selected as candidate events and a ring fit was then performed. A signal region ("road") was defined around the average ring radius from all selected events, with a width of ± 3 pixels for nitrogen and ± 1.7 pixels for C_4F_{10}. A three-pixel road corresponded to an angular spread of 7.5 mrad, meaning that the beam divergence, which was limited by the scintillator acceptance, was negligible with respect to the road definition. Hits outside the road were considered to be background. Events with four or more hits inside the road and two or less hits outside the road were selected for further analysis.

4.1. *Determining the Yield*

For a given run configuration, the average number of detected photo-electrons was extracted from a fit to the number of hits inside the road for selected events, using the procedure described in detail by M. Adinolfi *et. al.* [8]. Figure 2 shows an example of such a fit for a nitrogen radiator, with the fit function broken down into species of component particles. The fit included a term modeling pixel-to-pixel charge sharing, where a single photo-electron produces charge in two adjacent pixels, resulting in two hits. The procedure to determine the charge sharing term is described in Section 4.2. Also included in the fit was a term to model the probability that two photo-electrons within the Cherenkov ring strike the same pixel. Additional terms were included to model the relative abundances of $\bar{p}$, of K^- and the combined abundances of e^-, π^- (both saturated) in the beam and the relative photon yields expected from each. Finally there was provision for up to three incident particles per event.

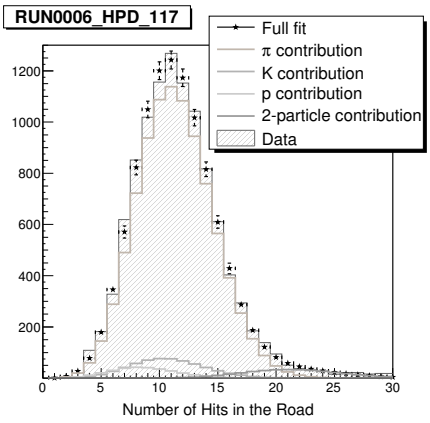

Fig. 2. The number of hits within the photo-electron road for the nitrogen radiator (points) compared to the fit (histograms).

4.2. *Charge Sharing*

The pixel-to-pixel charge sharing probability is defined as the probability that a single photo-electron striking the anode will result in two adjacent hits. The probability that i charge shares occur in an event with n hits is then modeled by a Poisson distribution with mean $(n-i)s$, where s is the charge sharing probability.

The charge sharing probability was independently measured in isolation from the beam, using an LED light source that provided a uniform illumination of the HPDs. The LED intensity was tuned to produce an average of four photo-electrons per HPD per event. Adjacent pixel hits were used to form a cluster of hits. In order remove ion feedback [1] events, all LED events with more than five clusters in an HPD, or at least one cluster of size > 2, were ignored. The number of adjacent hits remaining are assumed to originate from charge sharing plus a contribution from two genuine photo-electrons striking adjacent pixels (two photo-electron contribution).

A "toy" model was developed to simulate pixel hits in an LED run in the absence of charge sharing. Hits were distributed randomly over an area on the HPD pixel chip defined by the projection of the active area of the photo-cathode. By normalising the number of hits to real data, the number of adjacent hits in the toy model was then used to estimate the two photo-electron contribution to the LED data.

The estimated two photo-electron contribution is then subtracted from the measured number of adjacent hits. The charge sharing probability is the ratio of the remaining number of adjacent hits to the total number of clusters (including single hits).

In this way the charge sharing probability was found to be in the range $2-5\%$ for the HPDs in the test beam.

4.3. *Results with Nitrogen Radiator*

The photo-electron yields in nitrogen were studied with the Cherenkov rings focused onto several individual HPDs. There are a number of contributions to yields in C_4F_{10} that are unimportant in nitrogen. The Cherenkov photons produced at any radial angle within nitrogen can always be focused within the acceptance of a single HPD; the variation of the HPD quantum efficiency (QE) over a single HPD is always less than across multiple HPDs. In nitrogen, there are no alignment effects of HPDs to consider, only the mirror alignment has a significant contribution. Hence nitrogen runs formed a control for C_4F_{10}.

The expected yields per HPD were determined analytically. The uncertainty on the expected yield

[1] The HPD can occasionally experience ion feedback, where a photo-electron collides with an ion within the HPD vacuum envelope which then drifts slowly back to the photo-cathode and results in the ejection of typically 20 electrons. These electrons are accelerated to the anode where they create a large cluster of neighboring hits.

was dominated by the uncertainties in the product of the QE, mirror reflectivity and transmission coefficients of the quartz windows (QRT). Table 1 shows the number of hits per event with the previously mentioned cuts applied. The results were in good agreement with expectations.

Table 1
Measured and expected photo-electron yields (n.p.e) for nitrogen data. The HPD numbers are simply labels defined at production.

HPD number	Measured n.p.e	Expected n.p.e
117	12.32 ± 0.12	12.2 ± 0.6
264	13.14 ± 0.13	14.1 ± 0.7
265	12.56 ± 0.12	12.8 ± 0.7

4.4. *Results with C_4F_{10} Radiator*

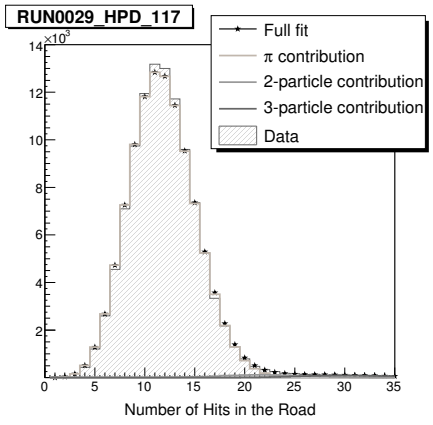

Fig. 3. The number of hits within the photo-electron road for the C_4F_{10} radiator (points) compared to the fit (histograms).

Runs were taken with the C_4F_{10} radiator, with Cherenkov rings focused on either three or four HPDs. The expected yields were determined using the GEANT4-based LHCb simulation package [10] with a modified geometrical description for the test beam. Ring fits were performed per HPD segment. The figure of merit for the detector was the photo-electron yield per radian, shown in Table 2. The average yield was 9 p.e/rad, with a 10% spread between HPDs, being consistent with the measured QE variation. The uncertainty on the expected yield was again dominated by the uncertainty in the assumed QRT.

Table 2
Measured and expected photo-electron yields per radian for C_4F_{10} data. The HPD numbers are simply labels defined at production.

HPD Number	Measured n.p.e/rad	Expected n.p.e/rad
117	8.5 ± 0.4	9.2 ± 0.5
265	8.8 ± 0.3	8.2 ± 0.5
282	9.4 ± 0.6	9.6 ± 0.5
283	9.2 ± 0.6	7.8 ± 0.4

4.5. *Systematic Errors*

Systematic uncertainties relating to various parts of the analysis were estimated. With C_4F_{10} runs, the definition of the size of the photo-electron road was varied between 1.5 and 3 pixels, the three particle term removed, the fit model changed to simple binomial-like, and the fit range varied. The largest systematic contribution to the photo-electron yield was from the photo-electron road definition, namely $1 - 4\%$. The systematic errors are therefore conservatively estimated to be at the 5% level.

5. Summary

A set of three production columns of HPDs from the LHCb RICH 2 sub-detector, including final readout electronics, has operated successfully with the LHC bunch structure and final data acquisition. Photo-electron yields are within expectations and satisfy LHCb requirements. The Cherenkov angle resolution is currently under study.

References

[1] LHCb Collaboration, *LHCb Technical Proposal, CERN/LHCC* 1998 004.
[2] LHCb Collaboration, *LHCb Re-optimised TDR, CERN/LHCC* 2003 030.
[3] LHCb Collaboration, *LHCb RICH TDR, CERN/LHCC* 2000 037.
[4] T. Gys, *et al.*, *Nucl. Instr. and Meth. A* 465 (2001) 240.
[5] K. Wyllie *et al.*, *Nucl. Instr. and Meth. A* 530 (2004) 82. K. Wyllie, *et al.*, *Proceedings of the Fifth Workshop on Electronics for LHC Experiments, Snowmass* 2024 CERN/LHCC/99-33.
[6] M.Adinolfi *et al.*, *Nucl Inst. and Meth. A* 572 (2007) 689.
[7] S. Wotton *et al.*, *CERN EDMS 768873* 2006-08-23.
[8] M. Adinolfi *et al.*, *Nucl Inst. and Meth. A* 574 (2007) 39.
[9] T. Gys *et. al.*, *Nucl Inst. and Meth. B* 285 (2004) 66.
[10] S. Agostinelli *et. al.*, *Nucl Inst. and Meth. A* 506 (2003) 250.